Stability of giant vortices in quantum liquids

Christophe Josserand

Laboratoire de Modélisation en Mécanique,

UPMC-CNRS UMR 7607, Case 162, 4 place Jussieu,

75005 Paris-France

We show how giant vortices can be stabilized for strong external potentials in Bose-Einstein condensates. We illustrate the formation of these vortices thanks to the Ginzburg-Landau dissipative dynamics for two typical potentials in two spatial dimensions. The giant vortex stability is studied for the particular case of a rotating cylindrical hard wall. Due to axial symmetry the minimization of the perturbed energy is simplified into a one dimensional relaxation dynamics. Solving this 1D minimization problem, we observe that giant vortices are either never stable, or only stable in a finite frequency range. Finally we obtain the marginal curve for the minimum frequency needed to observe a giant vortex.

Keywords: Bose-Einstein condensates, quantized vortex, multiple charge, energy minimization.

Quantised vortices are characteristics of quantum systems. Their circulation is quantised and they appear for instance when a rotation is imposed on a quantum liquid. We study here the conditions under which vortices with multiple charges can be observed. It is in general not possible since the energy of an array of single vortices is below the energy of a multiple vortex with the same total circulation charge. However an opposite trend appears if the system is confined. Indeed, in a confined system, an array of vortices generates an higher surrounding bulk density than the equivalent giant vortex. Thus the contribution to the nonlinear energy term penalizes now the vortex array and the balance between these two effects may allow the stability of giant vortices. In particular, this is the case for recently achieved Bose-Einstein condensates where an optical trap maintains the gas in a small volume. We show that if the trap potential is strong enough, the multiply charged vortex becomes stable. The linear stability of these giant vortices is performed using one dimensional minimization

techniques.

INTRODUCTION

The recent achievement of Bose-Einstein condensates (BEC)[1–3] has strongly renewed and restimulated interest in the numerous theories of quantum gases/liquids. By their lower densities, their larger healing lengths, the BEC presents important advantages compared to the traditional Helium superfluid, regardless of the fundamental interest of the Bose-Einstein transition itself. One of the striking properties of these quantum gases/liquids is the quantization of the vorticity[4]. It manifests itself through the formation of vortices whose circulation is quantised in units of $\hbar/m$, where m is the mass of an atom of the gas and $\hbar$ is the Planck constant. Such vortices have been observed in BEC by two different procedures in recent years[5–7]. Firstly[5] by rotating the BEC using laser techniques. This experiment is the analogy of the famous rotating bucket of superfluid helium where the first direct observation of quantized vortices was obtained[8]. The vortices appear suddenly as the rotation frequency increases, either one by one, or in groups, depending on the experimental procedure. The other experiment[6, 7] exploits the dynamical transition to vortex shedding of an accelerated superflow[9]. Experimentally, to achieve the BE condensation the atoms of the condensate have to be placed in an optical trap which creates an effective (mostly harmonic) confining potential. In the above experiments only single charged vortices were observed and no multicharged vortices (called a giant vortex of charge q or q-vortex later on) were detected. However, by imposing specific initial states, it has been possible to observe metastable long-lived giant vortices experimentally [10]. It is actually well known that multicharged vortices are always dynamically and thermodynamically unstable in homogenous and infinitely large quantum liquids[11]. This result is deduced from an energetic comparison between the multiply charged vortex and the vortex array. Due to the kinetic energy term, the giant vortex is found to be a local maximum of the free energy of the system. When the system is confined in a trap potential, the situation becomes more tricky since the potential encourages vortex merging while the vortices try to expand the condensate. In fact, the vortex array creates low density regions (one for each vortex) so that the surrounding bulk has to have higher density than for a multiply charged vortex. Thus, the nonlinear energy term is enhanced by a vortex array. If a large enough number of vortices is considered, this can compensate the kinetic energy effect and giant vortices become stable. For BEC in a harmonic trap, variational stability analysis suggests indeed the existence of a critical frequency above which the giant vortex should be energetically favoured over the lattice of single vortices[12]. This critical frequency was however found to be higher than the frequency of the quadratic trapping potential. At such speed, the condensate is therefore unstable since the centrifugal force overcomes the trap confinement. This explains why no stable giant vortices can be observed in rotating BEC if only harmonic trap are experimentally considered. This peculiar property of harmonic confinement does not actually prevent the stability of giant vortices for stronger trap potentials. In fact different groups have shown numerically and argued analytically that giant vortices are stable for high enough rotation if the trap potential is taken stronger than harmonic[13–16]. Numerical simulations have exhibited these giant vortices and some coexistence diagramms were even obtained[13, 14], although no clear stability arguments were presented. Recently, three dimensional formation of multiply charged vortices have also been numerically observed[15]. In the other work[16] the stability analysis was only performed in the framework of Wigner-Seitz approximation of a vortex lattice. Adequately strong trap potentials can be experimentally achieved thanks, for example, to Laguerre-Gaussian laser beams[17] but the experimental observation of stable giant vortices remains to be done.

In this note, we address the stability analysis of the giant vortices for the rotating cylinder. We use numerical simulations for two-dimensional systems subject to rotation $\mathbf{\Omega} = \Omega\mathbf{z}$, assuming translational invariance in the z-direction. The giant vortex formation is shown for illustration in a rotating BEC with quartic potential but we restrict thereafter our treatment to the case of an infinite cylindrical potential.

THE MODEL

The dynamics of a quantum Bose gas in the rotating frame in two dimensions is described by the dimensionless Gross-Pitaevskiĭ (G-P) equation[18–20]:

$$i\partial_t\psi = \left(-\frac{1}{2}\nabla^2 + V(r) + M|\psi|^2 + i\Omega\partial_\theta\right)\psi \tag{1}$$

where $\psi(\mathbf{r},t)$ is the condensate wave function normalized to unity: $\int d\mathbf{r}|\psi|^2 = 1$, $\mathbf{r}$ is the position vector (x, y), $r = |\mathbf{r}|$ and θ the corresponding cylindrical coordinates. The nonlinear strength $M = 4\pi Na$ is related to the product of the particle number per unit length, N, with the s-wave scattering length a. This dimensionless equation has in fact been deduced from the usual model using a typical length scale d that is defined by the trap properties. Consequently the length, energy and time in equation (1) are given in units of d, $\hbar^2/(md^2)$ and $md^2/\hbar$. The usual harmonic potential $\frac{1}{2}m\omega_t^2r^2$ leads to $V(r) = \frac{1}{2}r^2$ with $d = \sqrt{\hbar/(m\omega_t)}$. Below we restrict our work to two trap geometries. Firstly, for illustration, a quartic potential $\frac{m^2\omega_t^3 r^4}{\hbar}$, so that $V(r) = \frac{1}{4}r^4$ and $d = \sqrt{\hbar/(m\omega_t)}$ again. This potential has a smooth behavior and describes a stronger trap potential than the usual harmonic potential used in the experiments. The other potential models a quantum liquid entrapped in a cylindrical bucket of radius L. With $d = L$ the potential is described by $V(r) = 0$ if $r < 1$ and $V(r) = \infty$ otherwise. It corresponds to the well-known experiment on superfluid Helium where quantized vortices have been first vizualized[8]. Note that equation (1) admits only two control parameters for a given potential: the interaction coefficient M and the angular frequency Ω. The dynamics derives from a free energy F through: $\imath\partial_t\psi = \frac{\delta F}{\delta\psi^*}$ with:

$$F = \int d\mathbf{r} \left(\frac{1}{2}|\nabla\psi|^2 + i\Omega\psi^*\partial_\theta\psi + V(r) + \frac{M}{2}|\psi|^4 \right) \tag{2}$$

Stable equilibrium solutions of Eq. (1) correspond to local minima of F. The ground state is determined among the stable equilibrium solution as the one with the lowest energy . Stable equilibrium states of the condensate can be reached numerically through the dissipative dynamics of the Ginzburg-Landau equation. Formally it corresponds to an imaginary time evolution of the GP equation (1):

$$\partial_t\psi = -\left(-\frac{1}{2}\nabla^2 + 4\pi Na|\psi|^2 - \mu(N,\Omega) + V(r) + i\Omega\partial_\theta \right)\psi \tag{3}$$

We have introduced the chemical potential μ as the Lagrangian multiplier ensuring that the norm of ψ is unity. This time imaginary dynamics allows to reach a local minimum of the free energy close to the initial state and is useful to obtain the different stationnary solution of (1)[12]. Numerical simulations have been performed in two space dimensions up to 256×256 grid points. We have checked that numerical precision is not significantly affected by higher spatial discretizations for our range of parameters. Both Fast Fourier Transform (FFT) or finite difference methods have been used for spatial derivatives and again no dramatic changes were noticed between these schemes. The relative error in the normalization of the wave function was controlled to be below 10^{-3} and the precision for μ is better than 10^{-3}.

GIANT VORTEX FORMATION

To illustrate the formation of giant vortices, we follow numerically an equilibrium solution as Ω evolves. We start at $\Omega = 0$ with the ground state (vortex free solution) and we suddenly increase Ω by a small increment $\delta\Omega$. We retrieve an equilibrium state through the imaginary time dynamics (3) and the procedure is then iterated. Both the quartic and the hard-wall potentials are considered.

We first present the results for the quartic potential with $M = 12\pi$ (figures 1). Figure (1.a) shows the ground state solution, vortex-free at $\Omega = 0$. This solution survives without any change until $\Omega = 5.4$ where suddenly four vortices enter into the cloud (figure 1.b). They are well separated and form a square lattice. We observe also a spatial expansion of the cloud due to centrifugal effects. As Ω increases further on(figure 1 c)), the four vortices approach slowly the center of the trap. In this case the full merging of the four vortices is attained at $\Omega = 7.2$ (figure 1 d)), just before new vortices enter the cloud (at $\Omega = 7.35$).

A similar situation is observed for a superfluid in a cylindrical trap although in that case the condensate cannot expand when new vortices appear. Indeed we account for the infinite hard wall potential by imposing as boundary conditions $\psi = 0$ for $r \geq 1$. Figure (2) shows the density $|\psi|^2$ of the solution of equation (3) as Ω increases for $M = 300$. The shedding of four vortices occurs at $\Omega = 14.8$ (figure (2 a)) from the vortex free solution. Further increments of Ω lead to the convergence of the four vortices towards the center of the trap(figure (2 b)). But a different scenario arises here compared to the dynamics observed for the quartic potential. Indeed, before the four vortices collapse into a single 4-vortex, four new vortices are nucleated in the cloud at $\Omega = 20.8$(figure (2 c)). The condensate is now composed of a lattice of eight well separated vortices. Then new increases of Ω lead eventually to the merging into a giant 8-vortex at $\Omega = 26.2$ (figure (2 d)). Above this rotation, when new vortices are nucleated, they are immediatly absorbed by the giant vortex. This persistence of giant vortices for increasing frequencies has in fact been observed for all the numerical simulations that we have performed.

STABILITY ANALYSIS

For the sake of simplicity, the stability analysis is performed for the cylindrical wall trap potential. We want to know under which conditions a q-vortex is a local minimum of the free energy (2). We determine first the giant q-vortex states by seeking solutions of the form:

$$\psi_q^0(\mathbf{r}) = f_q(r)e^{iq\theta}$$

The trivial symetry of the problem $q \to -q$ with $\Omega \to -\Omega$ allows us to consider only the cases $q > 0$ from now on.

From the free-energy principle f_q has to satisfy:

$$\frac{1}{2}\left(f_q'' + \frac{f_q'}{r} - \frac{q^2}{r^2} f_q\right) - M f_q^3 + (\mu_q(M,\Omega) + q\cdot\Omega) f_q = 0 \tag{4}$$

$\mu_q(M,\Omega)$ is introduced again as the Lagrangian multiplier for the norm constraint $<\psi_q^0|\psi_q^0>=<f_q|f_q>= 2\pi\int r dr f_q^2 = 1$, where $<\cdot|\cdot>$ stands for the usual scalar product. The external potential term is replaced by the boundary condition $\psi = 0$ for $r \geq 1$. We observe from the preceeding equation (4) that the giant vortex solution f_q is in fact independant of Ω which only enters through the shift $\mu_q(M,\Omega) = \mu_q^0(M) - q\cdot\Omega$. These solutions are thus equilibrium states for all frequencies Ω regardless of their stability. The free energy of the vortex is written:

$$F_q = 2\pi \int r\cdot dr \left(\frac{1}{2}((f_q')^2 + \frac{q^2}{r^2} f_q^2) - q\Omega f_q^2 + \frac{M}{2} f_q^4\right) = T_q(M) + U_q(M) - q\cdot\Omega \tag{5}$$

Where $T_q(M) = \pi\int r\cdot dr((f_q')^2 + \frac{q^2}{r^2} f_q^2)$ is the kinetic energy and $U_q(M) = M\pi\int r\cdot dr f_q^4$ the nonlinear energy term. $E_q(M) = T_q(M) + U_q(M)$ is the total energy of the vortex solution. The q-vortex function f_q is found as before through the dissipative dynamics of the axisymmetric Ginzburg-Landau equation:

$$\partial_t f_q = \frac{1}{2}\left(f_q'' + \frac{f_q'}{r} - \frac{q^2}{r^2} f_q\right) - M f_q^3 + \mu_q^0 f_q \tag{6}$$

so that the equilibrium solutions f_q are local mimina of the free energy F_q. Figure (3 a)) shows the density f_q^2 of the solution for $M = 40\pi$ and $q = 0, 1, ..., 10$ as a function of the position r. As can be seen from equation (4), the bigger q, the larger the core of the vortex, and the higher is the density level outside the vortex core. Indeed, equation (4) for $r \to 0$ implies that the solution f_q behaves like r^q near the center. Figure (3 b)) represents also the $q = 5$ solution for M varying between 4π and 800π. The vortex core is shrinking as M increases in agreement with the evolution of the condensate healing length ($\propto 1/\sqrt{M}$) and so does the wall boundary layer.

Figure (4) shows the free energy of the giant vortices at $\Omega = 0$ as a function of q for different values of M. The energy is found to be a convex function of q for each curve. From this curve we can determine for each Ω which q-vortex minimizes the free energy. It defines an increasing set of critical frequencies $\Omega_q^m(M)$ such that the q-vortex is the one with the lowest energy for $\Omega_{q-1}^m(M) < \Omega < \Omega_q^m(M)$. It is then straightforward to obtain:

$$\Omega_q^m(M) = E_{q+1} - E_q$$

A q-vortex is stable when it is a local minimum of the free energy (2). We have seen in the full numerical simulation of the dissipative dynamics that such a vortex is unstable at low enough frequency Ω: it decomposes itself into q single vortices (see figures (1) and (2)). On the other hand, high frequencies destabilize the q-vortex by nucleating new vortices which gather into a new giant vortex as observed in the numerics. Thus, the q-vortex can only be stable in a finite range of frequency. Depending on the values of q and M, we may also observe that the q-vortex can be unstable for all values of Ω (it is the case for $q = 4$, $M = 300$ on figure (2)). The stability analysis is performed by an expansion of the free energy around the q-vortex solution. We write the perturbed wave-function of the giant vortex for $q > 1$ in the form:

$$\psi = \frac{\psi_q^0 + \delta\psi}{||\psi_q^0 + \delta\psi^q||}$$

Following the 2π periodic dependance in θ, we decompose the perturbation $\delta\psi^q$ among azimuthal modes as a Fourier set

$$\delta\psi^q(r,\theta) = \sum_{q'} \epsilon_{q'} g_{q'}^q(r) e^{iq'\theta}.$$

The complex functions $g_{q'}^q(r)$ describe the q' pertubation mode of the q vortex and are normalized to unity. The amplitudes $\epsilon_{q'}$ of the q' perturbation modes are complex numbers. We can omit the q perturbation mode which will bring nothing to the stability analysis since ψ_q^0 is already the minimizer of the axisymmetrical free energy with charge q. By analysing the perturbed wavefunction near $r = 0$, we observe that for $q' < q$ the perturbation mode describes the destabilization of the q vortex into a q'-vortex in the center surrounded by $q - q'$ single vortices. On the other hand, for $q' > q$ the perturbation describes the nucleation from the wall of $q' - q$ isolated vortices. We obtain for the perturbed wavefunction:

$$\psi = \frac{\psi_q^0 + \sum_{q' \neq q} \epsilon_{q'} g_{q'}^q(r) e^{iq'\theta}}{\sqrt{1 + \sum_{q' \neq q} |\epsilon_{q'}|^2}}$$

The free energy correction δF, at the first non-zero order in the ϵ's, is:

$$\delta F = \sum_{q' < q''} (\epsilon_{q'}, \epsilon_{q''}^*) \mathcal{L}_{q',q''} \begin{pmatrix} \epsilon_{q'}^* \\ \\ \epsilon_{q''} \end{pmatrix}$$

We omit the q superscript from now on. The set of operators $\mathcal{L}_{q',q''}$ follows:

$$\mathcal{L}_{q',q''} = \delta_{q'+q'',2q} \begin{pmatrix} \delta F_{q'} & 2\pi M \int r f_q(r)^2 g_{q'}(r) g_{q''}(r) dr \\ 2\pi M \int r f_q(r)^2 g^*_{q'}(r) g^*_{q''}(r) dr & \delta F_{q''} \end{pmatrix}$$

with the diagonal terms:

$$\delta F_{q'} = -T_q - 2U_q + (q - q')\Omega + 2\pi \int r dr \left(\frac{1}{2}((g'_{q'})^2 + \frac{(q')^2}{r^2} g^2_{q'}) + 2M \cdot g^2_{q'} f^2_q \right) \tag{7}$$

We notice here that the θ dependance of the free energy has been integrated so that further calculations will only concern the r spatial variations. This axisymmetric simplification leads eventually to a one dimensional stability problem. The stability of the q-giant vortex follows from the perturbed energy structure: if the operators $\mathcal{L}_{q',q''}$ are all found positive (*i.e.* that all its aigenvalues are positive) then the vortex is stable. On the other hand, if at least one of these operators is shown to have at least one negative eigenvalue the giant vortex is unstable either towards decomposition into simpler vortices or nucleation/annihilation of vortices. The operators $\mathcal{L}_{q',q''}$ in fact couple the two modes $g_{q'}$ and $g_{2q-q'}$ so that the determination of their full spectrum remains a complicated task.

However, if we could neglect the non-diagonal terms, the determination of the giant vortex stability would be straightforward. In such a case, the stability would only be determined by the minimization of the effective free energies $\delta F_{q'}$ associated with the functions $g_{q'}$ for each $q' \neq q$. Following this assumption, discussed in more detail below, we only have to determine the eigenfunction $\hat{g}_{q'}$ which minimizes the corresponding energy:

$$\delta E_{q,q'} = 2\pi \int r dr \left(\frac{1}{2}((g'_{q'})^2 + \frac{(q')^2}{r^2} g^2_{q'}) + 2M \cdot g^2_{q'} f^2_q \right) \tag{8}$$

with the following conditions (omitting the hat on the functions $\hat{g}_{q'}$ from now on):

$$< g_{q'} | g_{q'} >= 1. \;\; g'_0(0) = 0 \;\; g_{q' \neq 0}(0) = 0 \;\; g_{q'}(1) = 0 \tag{9}$$

We observe that the energy (8) is unchanged by the symetry $q' \to -q'$ so that we just need to calculate the minimizer for $q' \geq 0$. This corresponds to the calculation of a q' giant vortex placed into the effective potential:

$$U_{eff}(r) = 2M f_q(r)^2 + V(r)$$

The solution can be reached again through a dissipative dynamics:

$$\partial_t g_{q'} = \frac{1}{2}\left(g''_{q'} + \frac{g'_{q'}}{r} - \frac{q^2}{r^2} g_{q'}\right) - 2M f_q^2 g_{q'} + \mu' g_{q'} \qquad (10)$$

where μ' is introduced here as the Lagrangian multiplier for the unit norm constraint. Figure (5) shows precisely different $g_{q'}$ for $q = 4$ and $M = 300$. The q giant vortex profile is also indicated. As suggested by the effective potential, the perturbation modes are concentrated near the center of the trap for $q' < q$ where the giant vortex density is very small. For $q' > q$ the density $g_{q'}$ is concentrated near the wall since the centrifugal term of the perturbation dominates the q-vortex influence. These curves validate for $|q'| < q$ our assumption of weak off-diagonal terms made above. Indeed, the interaction term $g(q')g(2q - q')$ is very small there since one of the solutions is concentrated near $r \sim 0$ while the other is only present near $r = 1$. For $q' < -q$ we cannot draw conclusion so easily since both terms are concentrated near $r = 1$. We will assume in the following that we can still neglect the off-diagonal terms in these cases. When these terms are neglected for $q' < -q$, we will observe that the diagonal terms are then always positive, of higher and higher amplitude as $|q'|$ increases.

By minimizing the energy $\delta E_{q,q'}$ (8), we can determine whether the functional $\delta F_{q'}$ (7) is positive definite for a given frequency Ω. The sign of this free energy for the q'-perturbation changes at:

$$\Omega_c(q') = \frac{T_q + 2U_q - \delta E_{q,q'}}{q - q'}$$

It tells us that for $q' < q$ the q' perturbation mode is stable for $\Omega > \Omega_c(q')$ while for $q' > q$ it is stable only for $\Omega < \Omega_c(q')$. The change of inequality is due to the change of sign of $q - q'$. We then define two critical curves $\Omega_{low}(q') = \Omega_c(q')$ and $\Omega_{high}(q') = \Omega_c(2q - q')$ calculated both for $q' < q$. For a given Ω, if one can find a q' such that $\Omega_{low}(q') > \Omega$ then the q-vortex cannot exist since it decomposes into a more complex vortex configuration. On the other hand, if one can find a q' such that $\Omega_{high}(q') < \Omega$, the q vortex is also unstable and new vortices enter into the cloud. Thus the q-vortex can only be observed if $\mathrm{Max}_{q'<q}\Omega_{low}(q') < \mathrm{Min}_{q'<q}\Omega_{high}(q')$ and the q-vortex is linearly stable only for $\mathrm{Max}_{q'<q}\Omega_{low}(q') < \Omega < \mathrm{Min}_{q'<q}\Omega_{high}(q')$. In particular, if $\mathrm{Min}_{q'<q}\Omega_{high}(q') < \mathrm{Max}_{q'<q}\Omega_{low}(q')$ the giant vortex can never be observed since it would destabilize towards the shedding of new vortices before it becomes linearly stable towards decomposition. Figures (6) a) and b) show $\Omega_{low}(q')$ and $\Omega_{high}(q')$ for $M = 300$, $q = 4$ and $q = 8$ respectively. This is in qualitative agreement with the full numerical simulation. In figure (2) the four vortex

configuration destabilizes into a eight-vortex one at $\Omega = 20.8$. On the other hand, the stability analysis shows that the 4 giant vortex becomes unstable at $\Omega = 22.29$. This small discrepancy between these two frequencies can be explained by the fact that in one case we have a 4 single vortices configuration while the stability analysis concerns the giant vortex solution, saying nothing on the accuracy of the numerics.

Figure (7) presents the evolution of $\mathrm{Max}_{q'<q}\Omega_{low}(q') < \Omega < \mathrm{Min}_{q'<q}\Omega_{high}(q')$ for $q \in [2, 15]$. As observed above, it shows that for $q < 7$ no giant vortex can be observed while for $\Omega > 25.74$ giant vortices of charge $q > 6$ can be observed in a given range of Ω.

Defining $\Omega_g(M)$ (respectively $q_g(M)$) as the lowest frequency (vortex charge) at which a giant vortex can be observed for a strength M, we determine eventually in the Ω-M plane (or q-M plane similarly) the region where the solution consist in stable giant vortices only. The curves $\Omega_g(M)$ and $q_g(M)$ delimiting these regions are shown on figure (8). Interestingly, the best fit for the large M values suggest that $\Omega_g(M) \propto \sqrt{M}$ and similarly $q_g(M) \propto M^{2/3}$. Scaling arguments predicting these behavior in the asymptotic limit $M \to \infty$ are to be done.

DISCUSSION

We have shown numerically that giant vortex solutions can exist in an axisymmetric 2-D BEC model for trap potentials steeper than harmonic. We have investigated in more details the linear stability of these vortices for the cylindrical wall-like potential. The axial symmetry of the giant vortex simplifies the stability procedure into a one dimensional minimization problem which allows an almost analytical treatment. Under a no off-diagonal terms assumption, presenting good agreement with the full numerical studies we can determine the regions where the giant vortices are stable. We observe that for a given non linearity strength, one can always find a frequency above which only giant vortex configurations are ground state. Below this critical frequency, only single vortex lattices where observed. They become unstable to the shedding of new single vortices from the boundary before the equivalent giant vortex configuration can be linearly stabilized. Finally a master curve presenting the frequency and vortex charge above which giant vortices are stable for varying nonlinear strength M is presented. These results have been obtained for the particular case of cylindrical wall potential but can be adapted to smooth BEC potentials. The stability analysis leads to the same minimization problem but the numerical determination of the q' modes needs more careful investigation since they are not concentrated on $r \leq 1$ disk.

ACKNOWLEDGEMENTS

It is my pleasure to thank Vincent Hakim for his encouraging remarks on this work. I also would like thank warmly the editors for organising this special issue. I cannot also finish without express my special thanks to Yves Pomeau who made me discover the magic world of nonlinear dynamics!

REFERENCES

[1] C.C. Bradley, C.A. Sackett, and R.G. Hulet, Phys. Rev. Lett. **75**, 3969 (1995).

[2] M.H. Anderson, J.R. Ensher, M.R. Matthews, C.E. Wieman, and E.A. Cornell, Science **269**, 198 (1995).

[3] K.B. Davis, M.-O. Mewes, M.R. Andrews, N.J. van Druten, D.S. Durfee, D.M. Kurn, and W. Ketterle, Phys. Rev. Lett. **75**, 3969 (1995).

[4] R.J. Donnelly, *Quantized Vortices in Helium II* (Cambridge University Press, Cambridge, England., 1991).

[5] K.W. Madison, F. Chevy, W. Wohlleben, and J. Dalibard, Phys. Rev. Lett. **84**, 806 (2000).

[6] C. Raman, M. Khl, R. Onofrio, D. S. Durfee, C. E. Kuklewicz, Z. Hadzibabic and W. Ketterle, Phys. Rev. Lett. **83**, 2502 (1999).

[7] R. Onofrio, C. Raman, J. M. Vogels, J. R. Abo-Shaeer,A. P. Chikkatur and W. Ketterle, Phys. Rev. Lett. **85**, 2228 (2000).

[8] E.J. Yarmchuk, M.J.V. Gordon, and R.E. Packard, Phys. Rev. Lett. **43**, 214 (1979).

[9] T. Frisch, Y. Pomeau and S. Rica, Phys. Rev. Lett. **69**, 1644 (1992).

[10] P. Engels, I. Coddington, P.C. Haljan, V. Schweikhard, and E.A. Cornell, cond-mat/0301532 (2003).

[11] I.S. Aronson and V. Steinberg, Phys. Rev. B **53**, 75 (1995).

[12] Y. Castin and R. Dum, Eur. Phys. J. D **7**, 399 (1999).

[13] E. Lundh, Phys. Rev. A **65**, 043604 (2002).

[14] K. Kasamatsu, M. Tsubota, and M. Ueda, Phys. Rev. A **66**, 053606 (2002).

[15] A. Aftalion and I. Danaila, Phys. Rev. A 033608 (2004).

[16] U.R. Fischer and G. Baym, Phys. Rev. Lett. 140402 (2003).

[17] T. Kuga, Y. Torii, N. Shiokawa, T. Hirano, Y. Shimizu, and H. Sasada, Phys. Rev. Lett. **78**, 4713 (1997).

[18] E.P. Gross, J. Math. Phys. **4**, 195 (1963).

[19] L.P. Pitaevskiĭ, Sov. Phys. JETP **13**, 451 (1961).

[20] F. Dalfovo, S. Giorgini, L. Pitaevskiĭ, and S. Stringari, Rev. Mod. Phys. **71**, 463 (1999).

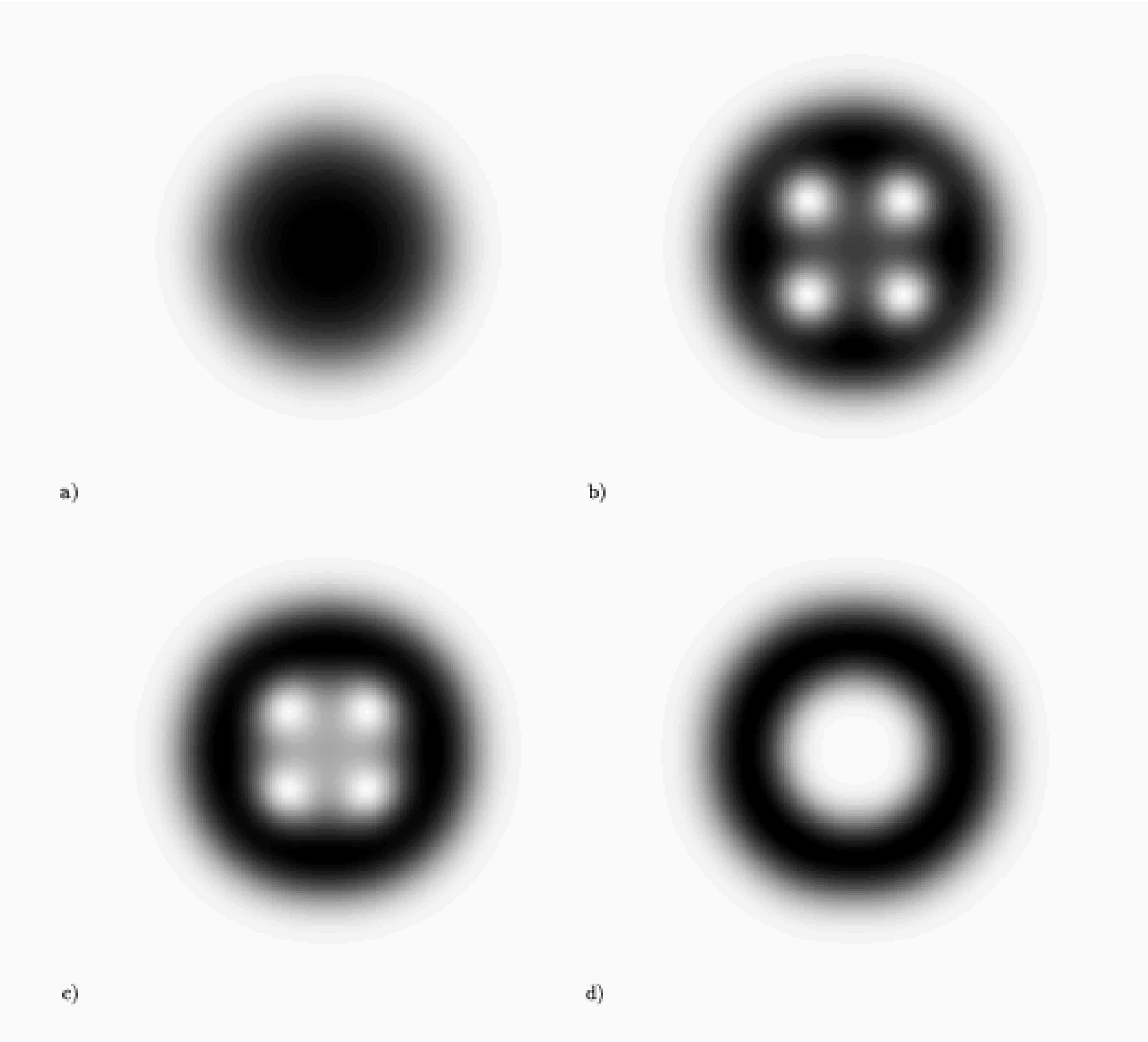

Figure 1: Quartic trap potential: density plots $|\psi|^2$ for $N \cdot a = 3$ at $\Omega =$ a) 0., b) 5.4, c) 6.6, and d) 7.2. The grid size is 128×128 and a pseudo-spectral method is used. The darker the color, the higher the density so that the vortices appear as white hole in the condensate.

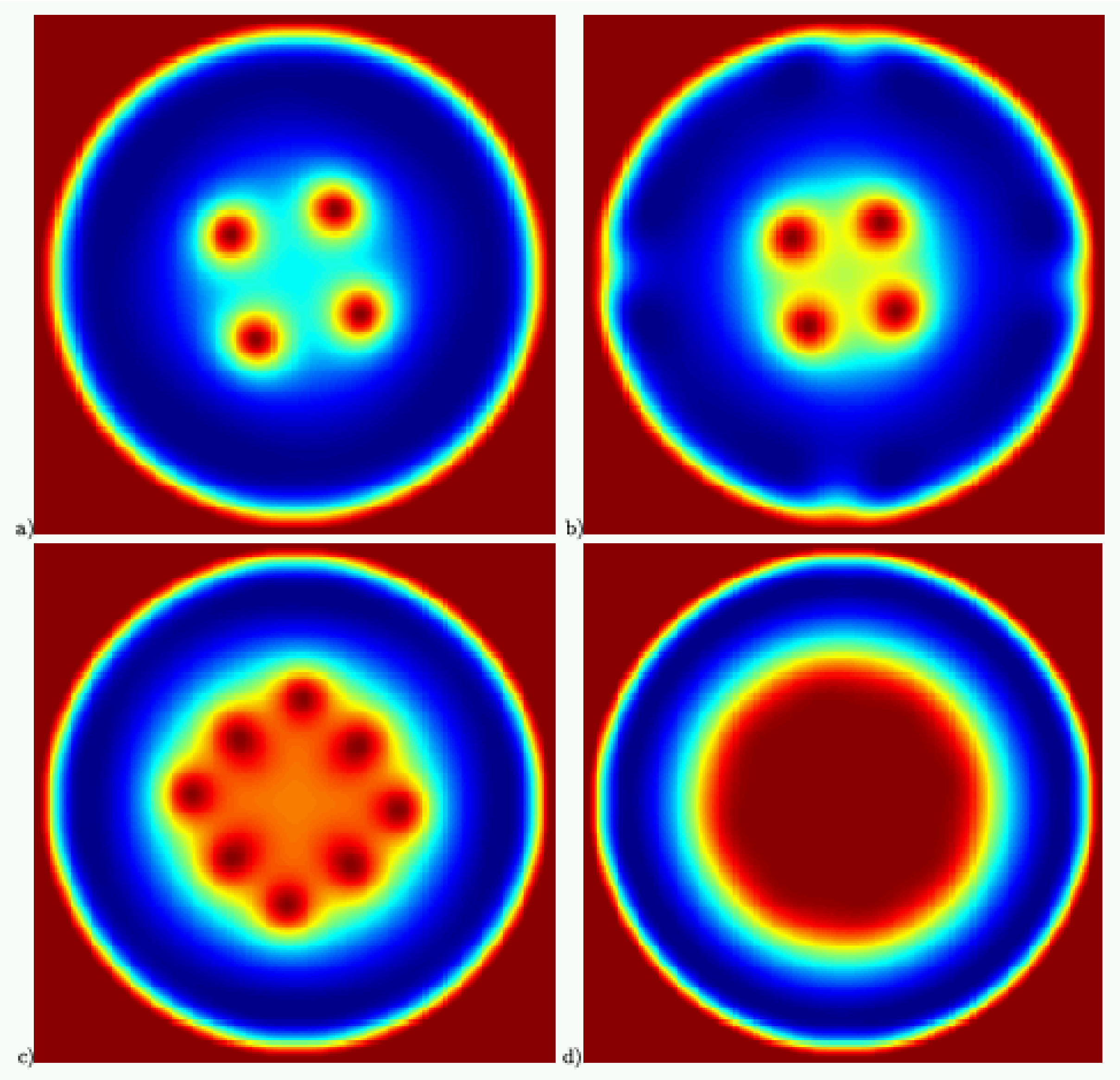

Figure 2: Density plots for $M = 300$, for $\Omega =$ a) 14.8, b) 18., c) 20.8, and d) 26.2. The grid size is 250×250 and the increment of the angular frequency is 0.2. The color scale goes from blue for zero density to red for the maximum density. The vortices appear as blue holes on the density field.

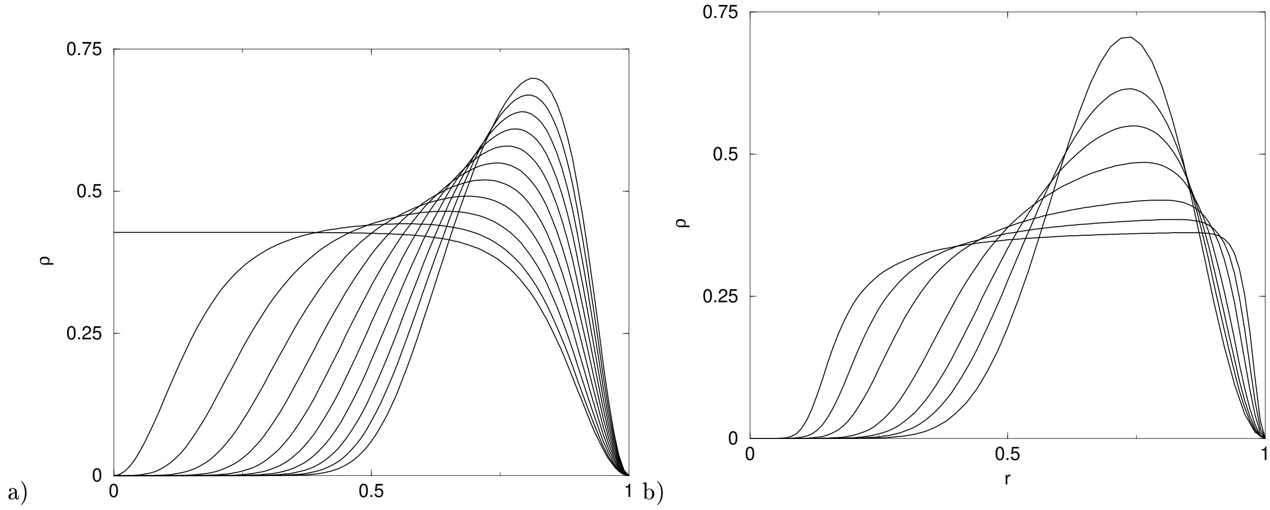

Figure 3: Density of the condensate f_q^2 for a) $M = 40\pi$ and $q = 0, 1...10$ b) $q = 5$ and $M/pi = 4, 20, 40, 80, 200$ 400 and 800; the higher the maximum of the curve, the smaller M and the bigger q. The profiles have been obtained as the stationnary solution of equation (6) and a regular grid of only 100 mesh points is needed for convergence.

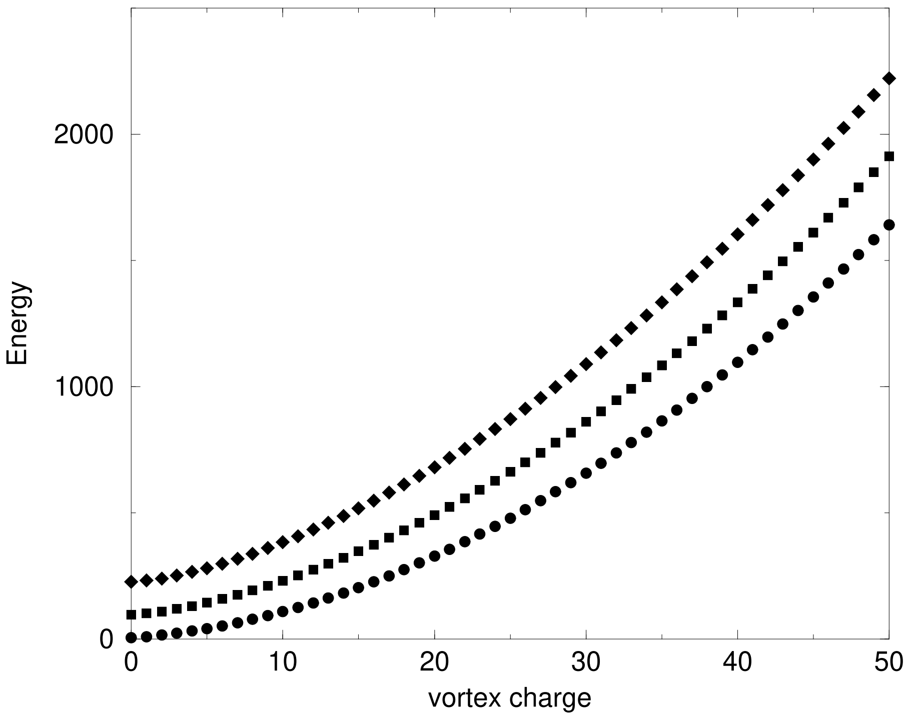

Figure 4: Energy of the vortex solutions as a function of the charge q for three different values of M. From bottom to top, $M = 1$ (circles), $M = 40$ (squares) and $M = 100$ (diamonds).

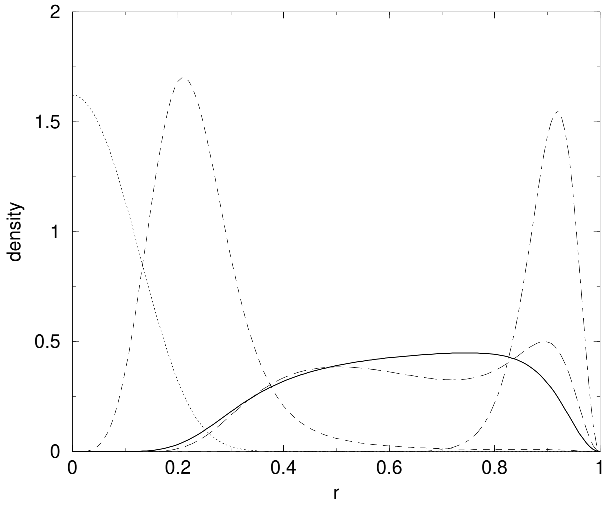

Figure 5: Density profiles of the perturbations modes $g_{q'}$ for a $q = 4$ giant vortex at $M = 300$. Only the profiles for $q' = 0$ (dotted line), $q' = 2$ (dashed line), $q' = 6$ (long dashed) and $q' = 20$ (dot-dashed) are indicated. The $q = 4$ vortex profiles is also shown (solid line). The density for $q' = 0$ and $q' = 2$ have been divided by height and two respectively for simplicity.

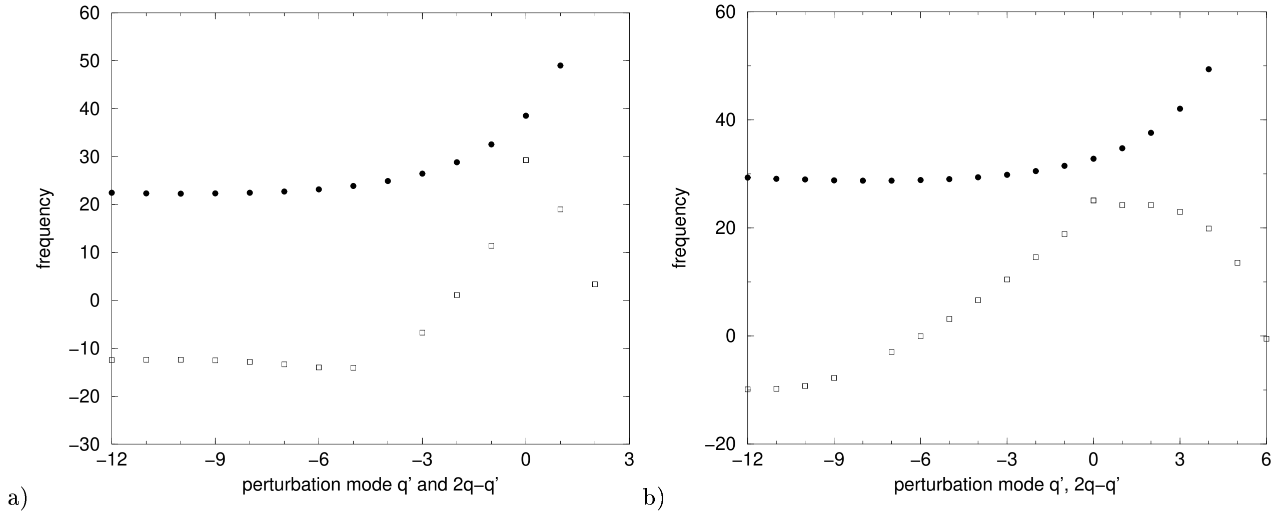

Figure 6: $\Omega_{high}(q')$ (black circles) and Ω_{low} (squares) as functions of the mode number q' for $M = 300$, a) $q = 4$, and b) $q = 8$. It illustrates the two generic situations encountered for the stability of a q-giant vortex: a) the 4-giant vortex is never stable; b) the 8-giant vortex is stable for Ω in the range $[25.09, 28.76]$.

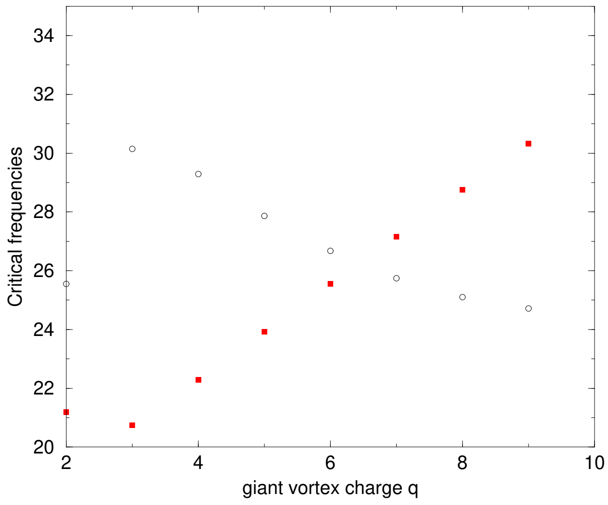

Figure 7: Evolution of $\mathrm{Max}_{q'<q}\Omega_{low}(q')$ (circles) and $\mathrm{Min}_{q'<q}\Omega_{high}(q')$ (red squares) for the giant vortex charge q between 2 and 15. The two curves cross between $q = 6$ and $q = 7$, so that only above $\Omega = 25.74$ can giant vortices be observed.

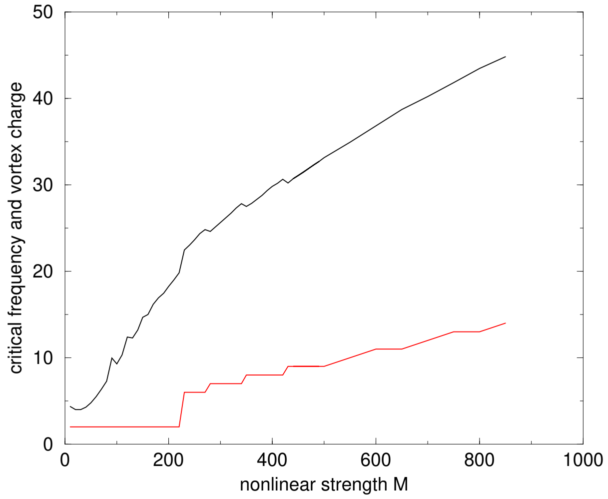

Figure 8: Critical curves $\Omega_g(M)$ (black line) and $q_g(M)$ (red line). Giant vortices are linearly stable above these curves.